LCOS-Based 3 × 3 Folded Wavelength Selective Switch With High-Resolution Spectral

Bing Yu, Yunshu Gao, and Genxiang Chen

***Abstract*—We propose and experimentally verify a 3 × 3 folded wavelength selective switch (WSS) scheme based on liquid crystal on silicon spatial light modulator (LCOS-SLM). This scheme adopts a concise double-layer folded structure that greatly reduced the structural complexity of the WSS system by using the same set of optical elements to accomplish twice beam deflection. The presented WSS is for the C-band, insertion loss is less than 13.2 dB, the spectral resolution is 1 GHz, the bandwidth tuning range is 16.25∼3750 GHz.**

***Index Terms*—Liquid crystal on silicon spatial light modulator, spatial light design, wavelength selective switch.**

I. Introduction

THE M×N wavelength selective switch (WSS) is one of the core optical components of the new generation of reconfigurable optical add/drop multiplexer (ROADM) [1], [2], [3], [4] and optical cross-connect (OXC) [5], [6], [7], can greatly reduce the construction, operation and maintenance costs of multi-dimensional optical nodes. In addition, the accurate spectral manipulation capability of M × N WSS can greatly improve the network expansion function and networking flexibility of optical nodes. In an M × N WSS, each wavelength signal from M input ports needs to be switched to N output ports. It is necessary to realize twice beam deflection inside the WSS, so M × N WSS faces the problems of complex structure, high insertion loss, and low accuracy of spectral manipulation.

The current M × N WSS technology is mainly divided into the following two types: One is a hybrid WSS system that combines WSS technology based on Planar Lightwave Circuit (PLC) technology and spatial light modulation technology [8]. But this system has large insertion loss, about 21 dB. The other is the WSS system based on liquid crystal on silicon spatial light modulator (LCOS-SLM) [9], [10], [11], [12], [13]. Fontaine et al. [9] presented LCOS-based 5 × 5 WSS in 2012, insertion loss in extreme cases exceeds 20 dB. Xiao et al. [10] presented 2 × 3 WSS in 2013, the spectral resolution is only 6.5 GHz, then it cannot accurately turn the channel center wavelength. Zong et al. [11] presented 8 × 8 WSS in 2015, the maximum insertion loss exceeds 20 dB. Xie et al. [12] presented 3 × 4 WSS in 2017, the 3 dB bandwidth tuning accuracy is only 6.25 GHz, doesn't have the ability to flexibly allocate channel bandwidth. Yuan et al. [13] presented 8 × 16 WSS in 2019, the minimum channel bandwidth is 50 GHz, the bandwidth tuning range is not ideal. Therefore, the M×N WSS with low insertion loss, high operating spectral resolution, and flexible transmission bandwidth has become the research focus of current research in the optical communication industry.

In this letter, we presented and experimentally verified a LCOS-based folded 3×3 WSS scheme that use one LCOS chip to realize wavelength switching between 3 input/output ports. Compared with the folded scheme proposed by Fontaine et al. [9], we use a high resolution LCOS and a symmetrical optical structure to improve spectral resolution and reduce insertion loss effectively. The WSS system proposed in this paper uses LCOS to control the size of the input/output beam in the port direction, so our WSS system can eliminate the need for a lens between two LCOS. The insertion loss of the whole system is less than 13.2 dB; the spectral resolution is 1 GHz; the 3 dB bandwidth tuning accuracy is 0.875 GHz; the bandwidth tuning range is 16.25∼3750 GHz. This scheme can achieve accurate spectral manipulation and flexible bandwidth allocation.

II. Methods

The basic schematic diagram of the presented WSS is shown in Fig. 1, the whole system structure can be divided into three parts: input module, port switching system and output module. For the input module, firstly, three incident beams from the fiber collimator array are expanded into approximately parallel light in the wavelength direction (x-direction) by the cylindrical lens pair-1. Then, the incident beam is demultiplexed by a diffraction grating, light have different wavelengths diffract according to corresponding diffraction angles. Next, the light beam will be focused on the LCOS in the wavelength direction after passing through the cylindrical lens 1. The compressed beam then reaches the port switch module, is deflected in the vertical direction (y-direction) by input LCOS. After the optical signal deviates from the original direction, it passes through the cylindrical lens 2 and the grating to reach the reflector for reflection. Then pass the grating and cylindrical lens 3 for the third time, reach the output LCOS for secondary pointing, make the beam propagate horizontally in the y-direction. Finally, the

Manuscript received 27 October 2022; revised 15 December 2022; accepted 27 December 2022. Date of publication 2 January 2023; date of current version 12 January 2023. This work was supported by the International Cooperation and Exchange of the National Natural Science Foundation of China under Grant 61960206013. *(Corresponding author: Genxiang Chen.)*

The authors are with the Engineering Research Center of Photonic Design Software, Ministry of Education, Beijing 100081, China, and also with the School of Science, Minzu University of China, Beijing 100081, China (e-mail: 18257163776@163.com; gaoyunshu@126.com; gxchen@muc.edu.cn).

Digital Object Identifier 10.1109/JPHOT.2022.3233663

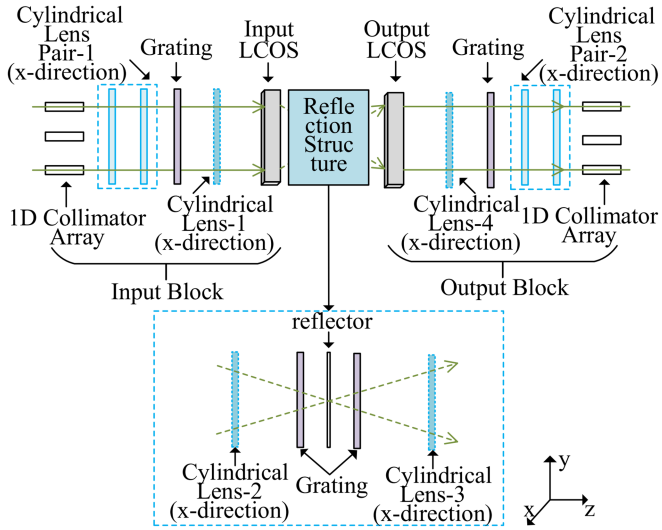

Fig. 1. Sequential structure of 3 × 3 WSS.

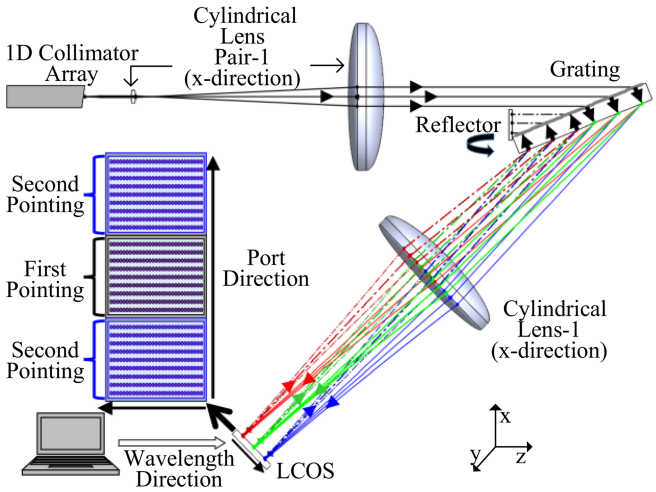

Fig. 2. Folded structure of 3 × 3 WSS.

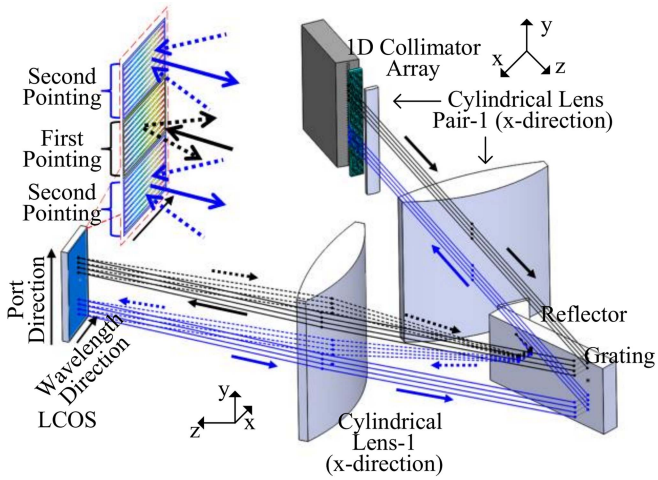

Fig. 3. Three-dimensional view of 3 × 3 WSS.

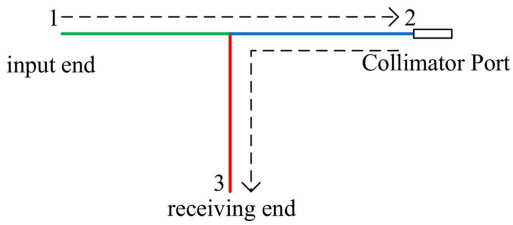

Fig. 4. Circulator schematic.

beam reaches the output module, passes through the cylindrical lens 4, the grating and the cylindrical lens pair-2 in turn, and finally reaches the output port.

Because the optical path of the presented system is highly symmetrical, we make each cylindrical lens reused by overlapping the front and rear optical paths, the structure is shown in Fig. 2. This structure can reduce the number of lenses and LCOS in the structure. The ideal reflector position coincides with the grating, it is impossible in practice. Therefore, the position of the reflector is moved backward and placed behind the grating. The entire LCOS is divided into three areas, corresponding to three ports. We define the LCOS region corresponding to the input port as the first pointing region, and the LCOS region corresponding to the output port as the second pointing region. Each of the three ports can be used as an input or output port, or both. Fig. 2 shows the case middle port is used as an input port and the ports on both sides are used as output port. In order to more clearly represent the folded structure of WSS, Fig. 3 presents a three-dimensional view of WSS. The ray traces for the upper port are omitted in the figure. Fig. 2 and Fig. 3 just showing a portion along the horizontal axis of the LCOS, the longer dimension of the LCOS is along the x-axis in next experiment. When a port is used as both an input and an output port, we use a circulator to separate the input and output signals, port 2 of the circulator is connected to the collimator port. The input signal is input from port 1 of circulator and then output to port 2. The output signal of WSS is input from port 2 of the circulator and then output to port 3, as shown in Fig. 4.

III. Experiment and Results

A. Construction of Wavelength Selective Switch System

According to the presented folded WSS structure, the experimental system shown in Fig. 5 was built. The LCOS-SLM used in the experiment is model GAEA from the Holoeye Germany. It is a phase only spatial light modulator. The resolution is 3840 × 2160, single pixel size is 3.74 μm. The long side of LCOS is placed along the wavelength direction. The groove direction of the grating is along port direction. The grating only disperses the incident light with TE polarization (the polarization direction is along the direction of the groove), the dispersion direction of the incident light passing through the grating is parallel to the long side of the LCOS. The LCOS only performs phase modulation on the incident light with TM polarization (the polarization direction is along the long side of the liquid

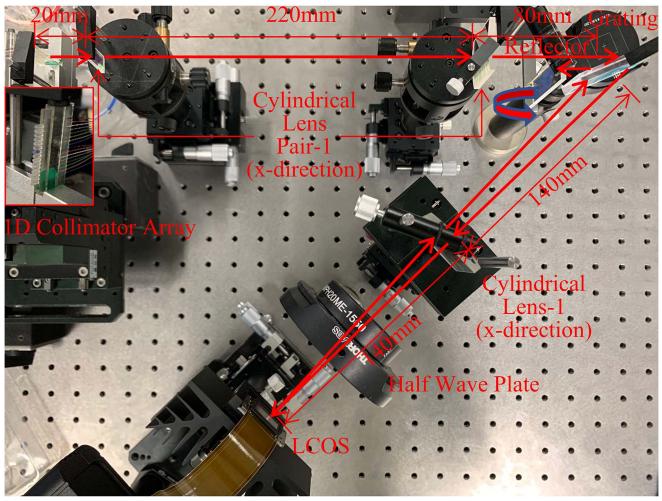

Fig. 5. 3 × 3 wavelength selective switch system.

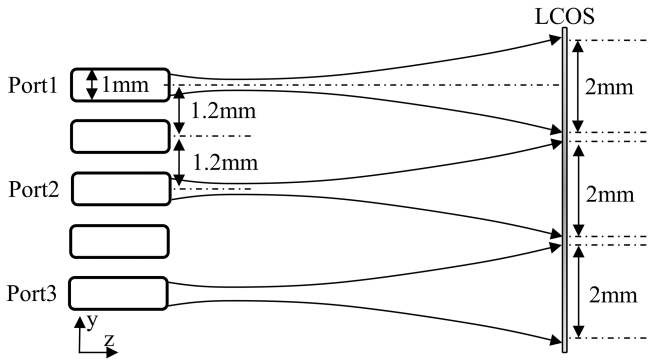

Fig. 6. Collimator Array Ports used.

crystal), so a half-wave plate needs to be placed between the liquid crystal and the grating to convert the incident light from TE polarization to TM polarization. In addition, gratings can only deal with TE polarized incident light, so the input light is the tuned TE mode line polarization light.

The input/output array is a 16-port 1D collimator array produced by Xuhai Opto-Electronic China, the port diameter is 1 mm and the spacing between adjacent ports is 1.2 mm. The beam diverges slightly after traveling a certain distance. The size of the light spot on the LCOS in the port direction is 2 mm when the light beam incident on the LCOS for the first time. It will lead to beams overlap of adjacent port, so use spacer ports as input/output ports, The collimator array ports used are defined as ports 1, 2, and 3, respectively, as shown in Fig. 6. Other component values are contained in Table I.

B. LCOS-Based Beam Manipulation Technology

When a port is used as both an input and an output port, we load a phase grayscale image to emulate a y-direction cylindrical mirror on the LCOS region corresponding to the port. The beam is focused on the y-direction (port direction) to ensure coupling efficiency when returning to the port. After testing, when the

TABLE I
VALUES FOR THE COMPONENTS

Component	Value
First lens of Cylindrical Lens Pair-1	Focal length: 20 mm
Second lens of Cylindrical Lens Pair-1	Focal length: 200 mm
Cylindrical Lens-1	Focal length: 140 mm
Reflector	Length: 40mm Width: 15mm
LCOS	Phase levels: 256 (8-bit) levels Fill factor: 90 % Reflectivity: 62% - 72% Illumination (max): ~ 2W/cm²
Grating	Duty cycle:0.5 Period: 833nm Number of lines:1200 lines/mm

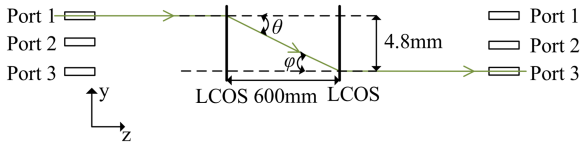

Fig. 7. Optical path model when switching ports.

focal length of the cylindrical lens is 210 mm, the beam coupling efficiency is the highest. When using different ports as input and output ports respectively, the phase grayscale image of the blazed grating that realizes deflection of the beam in y-direction is superimposed on the phase grayscale image of the simulated y-direction (port direction) cylindrical lens. Load the obtained phase grayscale image to the LCOS area corresponding to the input port for the first pointing. The width of one period of the blazed grating is represented by d. Define the angle φ between the incident light and the z-axis as the incident angle, the angle θ between the diffracted light and the z-axis is the diffraction angle, as shown in Fig. 7.

The diffraction angle of each level of diffracted light can be obtained by the grating equation:

$$d(\sin\varphi - \sin\theta) = n\lambda(n = 0, \pm1, \pm2\ldots) \tag{1}$$

In (1), $n = 0, 1, 2\ldots$represent the diffraction level. Take port 1 as the input port and port 3 as the output port as an example, the first pointing is completed after the incident light reaches the LCOS area corresponding to port 1, reflected light reaches the LCOS area corresponding to port 3 after transmitting 600 mm. In this process, the beam is deflected by 4×1.2 mm $= 4.8$ mm, corresponding deflection angle $\theta = 0.46°$. According to (1), the incident light is vertically incident, then incident angle $\varphi = 0°$. The required diffracted light is 1 level, then n $= 1$. The grating equation can be transformed into:

$$\theta = \arcsin\left(\frac{\lambda}{d}\right) = acr\sin\left(\frac{\lambda}{aN}\right) \tag{2}$$

Calculated by (2), the period size $d = 193.125$ μm. LCOS pixel size is $a = 3.74$ μm. Therefore, when the single period of the blazed grating phase grayscale image $N = 52$ pixels, the reflected light can be deflected to the LCOS area corresponding to the output port. In the second pointing, $\varphi = 0.46°$ and $\theta = 0°$.

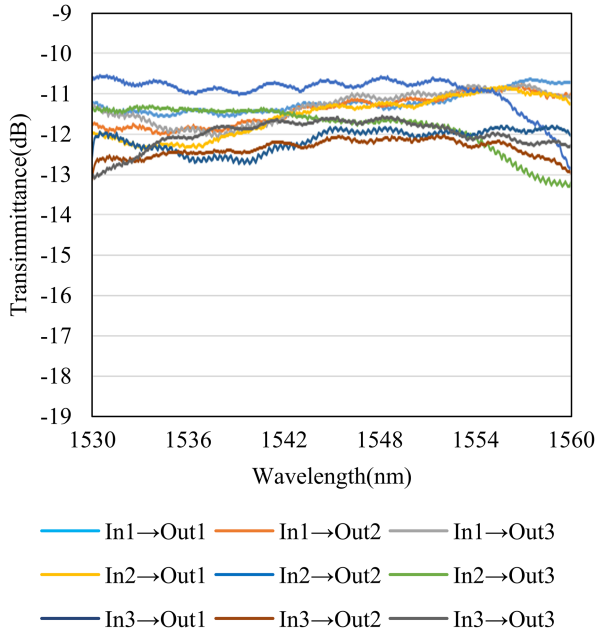

Fig. 8. Insertion loss testing.

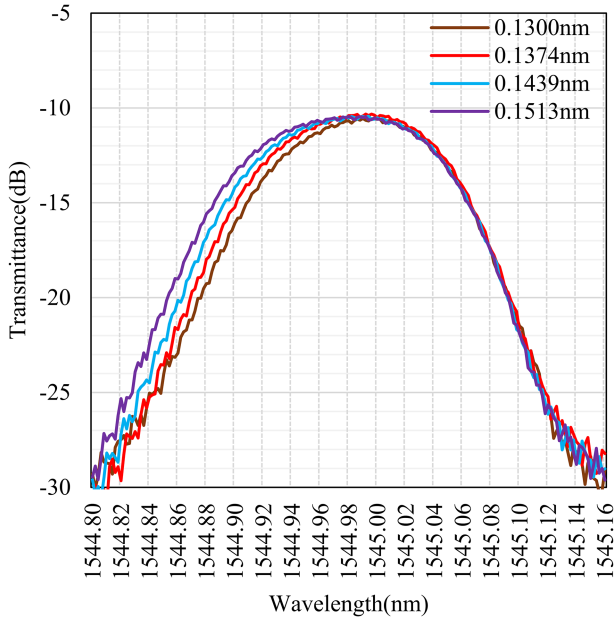

Fig. 9. 3 dB bandwidth tuning accuracy testing.

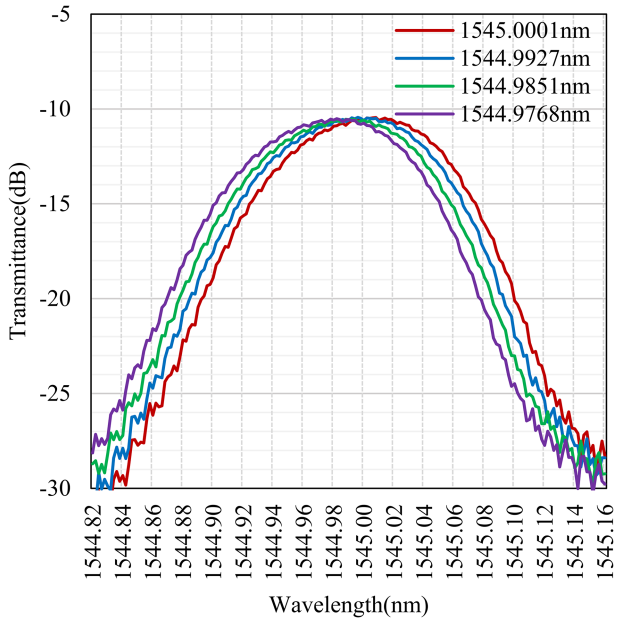

Fig. 10. Center wavelength tuning accuracy testing.

The period of the blazed grating grayscale image is the same as the first pointing.

C. Performance Testing

The amplified spontaneous emission (ASE) produced by an erbium-doped fiber amplifier (EDFA) as the input signal enter the complete WSS system. The AQ6370C spectrometer from YOKOGAWA was used as the signal receiving end. First, we connect EDFA and spectrometer directly to obtain ASE spectral density in the C-band. Next, the output spectral of WSS is subtracted from the ASE spectral, to get the final spectral data. The insertion loss and loss difference of the system can be observed more clearly in this way. Three collimator array ports are used as input and output ports simultaneously, all spectral data are plotted in the curves shown in Fig. 8 by measuring the insertion loss of the system. Although the loss of the entire WSS system within 13.2 dB is relatively large, the feasibility of this WSS system scheme is verified in principle. The beam output quality and the beam coupling efficiency can't be consistent, caused by the fiber collimator array manufacturing precision, these limitations result in a 3 dB difference in insertion loss.

The minimum channel bandwidth that WSS can achieve is determined by beam compression effect of cylindrical lens-1. The minimum channel bandwidth is tested by gradually decreasing the width of phase grayscale image on wavelength direction. Experiment show that the minimum channel bandwidth can be set to 0.1300 nm (16.25 GHz), the width of phase grayscale image along wavelength dispersion direction is 21 pixels at this time. As shown in Fig. 9, port 2 as the signal output port is selected to output one wavelength channel that is set with the 1545 nm center wavelength and 0.1300 nm 3 dB bandwidth. Then, the width of the phase grayscale image corresponding to this wavelength channel is controlled to increase by 1, 2, and 3 pixels sequentially. The corresponding channel 3 dB bandwidth increase is about 7pm (0.875 GHz), 14pm, 21pm. Therefore, WSS can arbitrarily adjust the 3 dB bandwidth of the output wavelength channel in an integer multiple of 7pm, and the bandwidth tuning accuracy less than 1 GHz.

WSS can precisely adjustment the center wavelength of the wavelength channel. 30 nm spectral width of the ASE light was mapped on the window of the LCOS. Therefore, each pixel accommodated a 30 nm/3840≈8pm bandwidth, which defines the WSS operating spectral resolution. The wavelength channel in Fig. 10, using port 2 as the input/output port, the

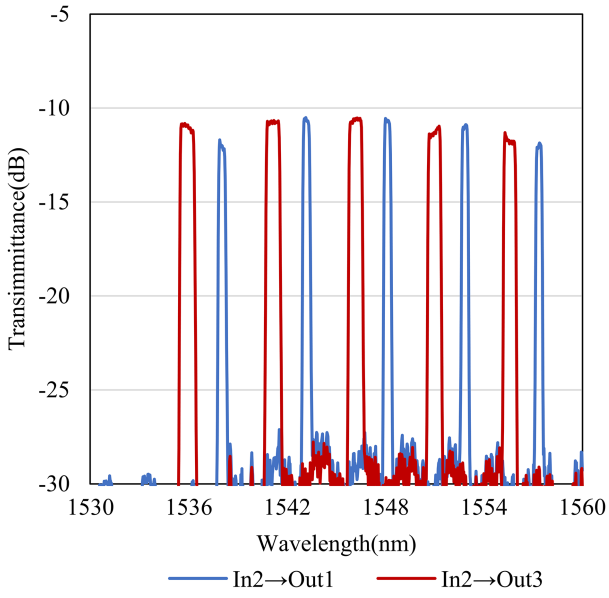

Fig. 11. Port 2 assigns channels to port 1 and 3.

3 dB bandwidth is 16.25 GHz. The center wavelength of the wavelength channel can be adjusted by switching different phase grayscale images. After measurement, the minimum tuning step size of the center wavelength of the wavelength channel is 8pm (1 GHz), and the minimum spectral tuning accuracy of the entire C-band is within the range of 8 ± 1pm, which defines the WSS operating spectral resolution. Therefore, this feature allows the WSS to arbitrarily set the center wavelength of each channel with an integer multiple of 8 ± 1pm.

The main function of the WSS is to switch any wavelength channel in the multi-wavelength incident light to any output port to realize signal exchange. As shown in Fig. 11, set port 2 as the input port, and at the same time assign five 50 GHz and five 100 GHz bandwidths to port 1 and port 3, respectively. The wavelength channels between the ports are not affected by each other. The origin of the light out of the bandwidths is crosstalk between ports, the crosstalk in the whole C-band is less than −27 dB.

IV. Conclusion

In this letter, we presented a LCOS-based 3 × 3 folded WSS. The maximum insertion loss of the presented wavelength selective switch system is less than 13.2 dB, the minimum spectral tuning accuracy is 1 GHz, and the bandwidth tuning accuracy is 0.875 GHz. The bandwidth tuning range is 16.25∼3750 GHz. This system can achieve accurate manipulation of the spectrum and flexible bandwidth allocation. The presented folded structure can greatly reduce the structural complexity of the WSS system.

In this system, the main factor limiting the number of ports is: There is no component to suppress the divergence of the beam in the port direction (y-direction) before the beam reach LCOS, the y-direction size of spot on LCOS exceeds the distance between adjacent ports. Therefore, LCOS can only accommodate three ports. We plan to reduce the focal length of cylindrical lens-1 in future work. This will reduce the distance between the collimator array and the LCOS, reduce the y-direction size of spot on LCOS accordingly. In addition, take the long side of LCOS with 3840 pixels as the port direction. By these means the system can be extended to a 12 × 12 WSS.

References

[1] B. P. Keyworth, "ROADM subsystems and technologies," in *Proc. OFC/NFOEC Tech. Dig. Opt. Fiber Commun. Conf.*, 2005, Art. no. 4.
[2] Q. She, Q. Zhang, and K. Rundberget, "CAPEX benefits of colorless directionless ROADM in WDM transport networks," in *Proc. Opt. Fiber Commun. Conf./Nat. Fiber Optic Engineers Conf.*, 2013, pp. 1–3.
[3] G. Shen, Y. Li, and L. Peng, "How much can colorless, directionless and contentionless (CDC) of ROADM help dynamic lightpath provisioning?," in *Proc. Nat. Fiber Optic Engineers Conf.*, 2012, pp. 1–3.
[4] C. Zhang, J. Li, H. Wang, A. Guo, and C. Janz, "Evaluation of dynamic optical service restoration on a large-scale ROADM mesh network," *IEEE Commun. Mag.*, vol. 57, no. 4, pp. 138–143, Apr. 2019, doi: 10.1109/MCOM.2019.1800307.
[5] X. Chen et al., "All-optical OXC transition strategy from WDM optical network to elastic optical network," *Opt. Exp.*, vol. 24, no. 4, Feb. 2016, Art. no. 4076, doi: 10.1364/OE.24.004076.
[6] M. Niwa, Y. Mori, H. Hasegawa, and K. Sato, "Tipping point for the future scalable OXC: What size M × M WSS is needed?," *J. Opt. Commun. Netw.*, vol. 9, no. 1, Jan. 2017, Art. no. A18, doi: 10.1364/JOCN.9.000A18.
[7] K. i. Sato, "How to create large scale OXCs/ROADMs for future networks," in *Proc. IEEE 16th Int. Conf. Transparent Opt. Netw.*, 2014, pp. 1–4.
[8] Y. Ikuma, K. Suzuki, N. Nemoto, E. Hashimoto, O. Moriwaki, and T. Takahashi, "8 × 24 wavelength selective switch for Low-loss transponder aggregator," in *Proc. Opt. Fiber Commun. Conf. Exhib.*, 2015, pp. 1–3.
[9] N. K. Fontaine, R. Ryf, and D. T. Neilson, "N × M wavelength selective cross connect with flexible passbands," in *Proc. IEEE Opt. Fiber Commun. Conf.*, 2012, pp. 1–3.
[10] F. Xiao and K. Alameh, "Opto-VLSI-based N × M wavelength selective switch," *Opt. Exp.*, vol. 21, no. 15, Jul. 2013, Art. no. 18160, doi: 10.1364/OE.21.018160.
[11] L. Zong, H. Zhao, Z. Feng, and Y. Yan, "8 × 8 flexible wavelength cross-connect for CDC ROADM application," *IEEE Photon. Technol. Lett.*, vol. 27, no. 24, pp. 2603–2606, Dec. 2015, doi: 10.1109/LPT.2015.2478796.
[12] D. Xie, Z. Liu, Q. You, and S. Yu, "Demonstration of a 3 × 4 tunable bandwidth WSS with tunable attenuation using compact spatial light paths," *Opt. Exp.*, vol. 25, no. 10, May 2017, Art. no. 11173, doi: 10.1364/OE.25.011173.
[13] Z. Yuan et al., "8 × 16 wavelength selective switch with full contention less switching," *IEEE Photon. Technol. Lett.*, vol. 31, no. 7, pp. 557–560, Apr. 2019, doi: 10.1109/LPT.2019.2902296.